The Astrophysical Journal, 871:39 (6pp), 2019 January 20 https://doi.org/10.3847/1538-4357/aaf575

Understanding the Limitations of Gyrochronology for Old Field Stars

Travis S. Metcalfe[1,2] and Ricky Egeland[3]
[1] Space Science Institute, 4750 Walnut Street, Suite 205, Boulder, CO 80301, USA
[2] Max-Planck-Institut für Sonnensystemforschung, Justus-von-Liebig-Weg 3, D-37077, Göttingen, Germany
[3] High Altitude Observatory, National Center for Atmospheric Research, P.O. Box 3000, Boulder, CO 80307, USA
Received 2018 September 28; revised 2018 November 20; accepted 2018 November 30; published 2019 January 21

Abstract

Nearly half a century has passed since the initial indications that stellar rotation slows while chromospheric activity weakens with a power-law dependence on age, the so-called Skumanich relations. Subsequent characterization of the mass-dependence of this behavior up to the age of the Sun led to the advent of gyrochronology, which uses the rotation rate of a star to infer its age from an empirical calibration. The efficacy of the method relies on predictable angular momentum loss from a stellar wind entrained in the large-scale magnetic field produced by global dynamo action. Recent observational evidence suggests that the global dynamo begins to shut down near the middle of a star's main-sequence lifetime, leading to a disruption in the production of large-scale magnetic field, a dramatic reduction in angular momentum loss, and a breakdown of gyrochronology relations. For solar-type stars this transition appears to occur near the age of the Sun, when rotation becomes too slow to imprint Coriolis forces on the global convective patterns, reducing the shear induced by differential rotation, and disrupting the large-scale dynamo. We use data from Barnes to reveal the signature of this transition in the observations that were originally used to validate gyrochronology. We propose that chromospheric activity may ultimately provide a more reliable age indicator for older stars, and we suggest that asteroseismology can be used to help calibrate activity–age relations for field stars beyond the middle of their main-sequence lifetimes.

Key words: stars: activity – stars: evolution – stars: magnetic field – stars: rotation – stars: solar-type

1. Background

Stars are born with a range of initial rotation rates and magnetic field strengths, and beyond the saturated regime the two properties are intricately linked for as long as a global dynamo continues to operate. The large-scale magnetic field gradually slows the rotation over time (e.g., see Réville et al. 2015; Garraffo et al. 2016). Through a process known as magnetic braking, charged particles in the stellar wind follow the magnetic field lines out to the Alfvén radius, shedding angular momentum in the process. In turn, nonuniform rotation modifies the morphology of the magnetic field (e.g., see Brown et al. 2010). Solar-like differential rotation, with a faster equator and slower poles, is a natural consequence of convection in the presence of substantial Coriolis forces (Miesch 2005). The resulting shear wraps up the large-scale poloidal field into a toroidal configuration that ultimately leads to the emergence of active regions on the surface. Through these basic physical processes, stellar rotation and magnetism diminish together over time, each feeding off the other. The mutual feedback can continue as long as rotation and magnetism are coupled through a global dynamo.[4]

Nearly half a century ago, Skumanich (1972) planted the observational seeds of this consensus view of magnetic stellar evolution. Both the theoretical foundations and the constraints from young clusters improved steadily over the intervening decades (e.g., see Soderblom et al. 1993, and references therein). But the Sun remained the oldest calibrator, so the empirical relations were largely untested beyond stellar middle-age. Barnes (2007) put forward a more quantitative formulation of the rotation-age relation (so-called *gyrochronology*), establishing the mass-dependence of stellar spin-down from observations of young clusters and using the Sun to determine the age-dependence. Given only the $B - V$ color and rotation period ($P_{\rm rot}$) of a star, gyrochronology yielded an empirical stellar age with a precision of 15%–20%. Barnes (2010) revised this formulation to account for varying initial conditions (P_0, important in young clusters), and to map the mass-dependence onto a convective turnover time (τ_c) derived from the stellar models of Barnes & Kim (2010). This approach more faithfully reproduced the distribution of rotation periods in young clusters, while yielding ages compatible with Barnes (2007) for more evolved stars.

Observations from the *Kepler* mission provided the first tests of gyrochronology for older clusters and for field stars beyond the age of the Sun. Meibom et al. (2011) found good agreement with expectations for the 1 Gyr cluster NGC 6811, and Meibom et al. (2015) extended this success to 2.5 Gyr with observations of the cluster NGC 6819. The first indications of unexpected behavior were uncovered by Angus et al. (2015), who found that no single gyrochronology relation could simultaneously explain the cluster data and the asteroseismic ages for old *Kepler* field stars with measured rotation periods. van Saders et al. (2016) confirmed anomalously fast rotation among the best characterized *Kepler* asteroseismic targets, and proposed a model that could explain the observations with significantly weakened magnetic braking beyond the middle of a star's main-sequence lifetime. Metcalfe et al. (2016) found the magnetic counterpart of this rotational transition in chromospheric activity measurements of the *Kepler* targets, showing empirically that the activity level continues to decrease while the rotation rate remains almost constant. They suggested that the transition might be triggered by a change in the character of differential rotation that was expected from global convection simulations (Gastine et al. 2014; Brun et al. 2017).

[4] By "global dynamo" we mean the mechanism that generates large-scale magnetic field, as opposed to a "local dynamo," which may generate field on smaller scales.

Metcalfe & van Saders (2017) identified a coincident shift in stellar cycle properties, with the cycle period growing longer and the amplitude becoming weaker at nearly constant rotation.

These developments suggest a revised picture of the late stages of magnetic stellar evolution, in which the disruption of differential rotation in the absence of substantial Coriolis forces leads to a gradual decrease in the production of large-scale magnetic fields by the global dynamo. The consequence of this transition is a decoupling of rotation and magnetism near middle-age, such that magnetic braking can no longer shed angular momentum efficiently and rotation remains almost constant until the subgiant phase. This scenario would also explain the long-period edge found by McQuillan et al. (2014) in the distribution of rotation periods with $B - V$ color for 34,000 stars in the *Kepler* field, where significantly longer rotation periods are expected from gyrochronology but not observed for solar-type stars (van Saders et al. 2018).

In an effort to address any skepticism about the existence of this transition, we identify its manifestation among the most evolved dwarfs in the Mount Wilson sample that were originally used to validate gyrochronology (Section 2). We then search within the *Kepler* asteroseismic sample to identify analogs of the Mount Wilson stars that show the largest inconsistencies between gyrochronology and chromospheric ages (Section 3), allowing us to characterize more precisely the decoupling of rotation and magnetism. In Section 4, we discuss future observations of these Mount Wilson stars with the *Transiting Exoplanet Survey Satellite* (*TESS*), and we predict that their asteroseismic ages will significantly exceed those expected from gyrochronology. We conclude in Section 5 with a discussion of the potential for reliable chromospheric ages of older stars, using asteroseismology to recalibrate the activity–age relation.

2. Gyrochronology Sample

After calibrating gyrochronology with young clusters and the Sun, Barnes (2007, hereafter B07) attempted to validate the method using a sample of bright field stars observed for decades by the Mount Wilson HK project (Wilson 1968). For the subset of 71 stars that were not known to be significantly evolved, B07 compiled $B - V$ colors, rotation periods $P_{\rm rot}$, and mean chromospheric activity levels $\log\langle R'_{\rm HK}\rangle$ from the literature (Noyes et al. 1984; Baliunas et al. 1996; Donahue et al. 1996). B07 then used the mean activity levels to calculate chromospheric ages from the activity–age relation of Donahue (1998), which could be compared to the ages and uncertainties from gyrochronology (see Table 3 of B07). Although Donahue (1998) did not provide a method for assessing uncertainties on the calculated ages, B07 noted that discrepancies in the age estimates for members of wide binaries and triple systems suggested a mean fractional error of 46%, about 3 times the typical age uncertainties from gyrochronology. In summarizing the comparison between the two age estimates, B07 noted in the abstract: "Gyro ages for the Mount Wilson stars are shown to be in good agreement with chromospheric ages for all but the bluest stars." Below, we use the data from Table 3 of B07 to reassess this comparison.

In Figure 1, we show the difference between the chromospheric and gyro ages, in units of the age uncertainty, plotted against the mean chromospheric activity level for 70 of the Mount Wilson stars tabulated in B07 (we omit only the M dwarf HD 95735, which has a spurious chromospheric age of

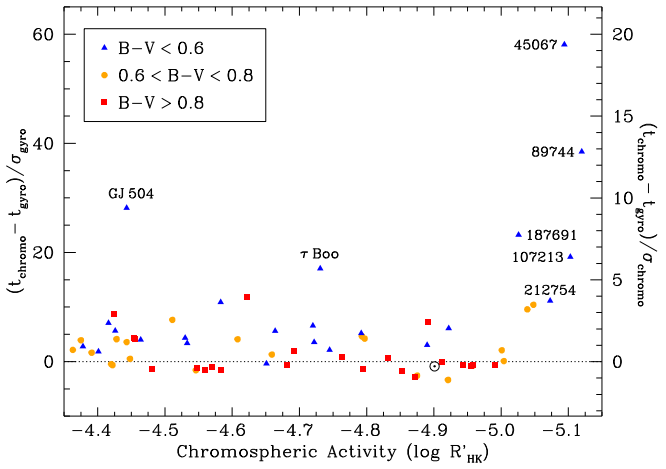

Figure 1. Difference between the chromospheric age and the gyro age, in units of the uncertainties ($\sigma_{\rm gyro}$ and $\sigma_{\rm chromo}$), for Mount Wilson stars at various activity levels. Data are taken directly from Table 3 of Barnes (2007). Colored symbols indicate hotter stars with $B - V < 0.6$ (blue triangles), solar-type stars with $0.6 < B - V < 0.8$ (yellow circles), and cooler stars with $B - V > 0.8$ (red squares), while the Sun is shown with its usual symbol (⊙). With the exception of two Jovian exoplanet host stars (GJ 504 and τ Boo), the two age estimates generally agree within $\sim 3\sigma_{\rm chromo}$ ($\sim 9\sigma_{\rm gyro}$) until the lowest activity levels ($\log R'_{\rm HK} < -5$) where rotation appears to decouple from activity (see the text for details). Most of these F- and G-type stars are classified as "Flat" or "Long" by Baliunas et al. (1995) from 25 years of Ca HK observations, suggesting that their global dynamos may already be shutting down, eliminating the large-scale fields that dominate magnetic braking. See Table 1 for numerical values of the age discrepancy for the outliers at low activity levels.

20 Gyr). On the left axis, the inconsistency between the age estimates is shown in units of the tabulated uncertainty on the gyro age, $\sigma_{\rm gyro}$. On the right axis, the values are scaled to reflect the larger uncertainty on the chromospheric age, $\sigma_{\rm chromo}$. Colored symbols separate the sample into hotter stars with $B - V < 0.6$ (blue triangles), solar-type stars with $0.6 < B - V < 0.8$ (yellow circles), and cooler stars with $B - V > 0.8$ (red squares). The solar values from B07 are indicated with the ⊙ symbol. As noted by B07: "apart from a slight tendency toward shorter gyro ages...there is general agreement between the chromospheric and gyro ages for this sample." With few exceptions,[5] the two age estimates tend to agree between activity levels of −4.3 and −5.0, in a band of uncertainty that stretches from −1 to +3 $\sigma_{\rm chromo}$ (−3 to +9$\sigma_{\rm gyro}$).

Given the relative precision of the two methods, we can assume that most of the scatter is due to the chromospheric age uncertainties. Although the median age inconsistency is indeed slightly higher for the blue stars ($B - V < 0.6$), the most significant outliers[6] are found at the lowest activity levels ($\log R'_{\rm HK} < -5$). These stars are labeled with their HD numbers in Figure 1, and their properties are listed in Table 1. There is reason to be skeptical of the chromospheric ages for these Mount Wilson stars. As pointed out by B07, the chromospheric ages for these stars exceed the main-sequence

[5] Exceptions include the two Jovian exoplanet host stars GJ 504 (Kuzuhara et al. 2013) and τ Boo (Walker et al. 2008), where the stellar rotation, activity, or both could plausibly be affected by interactions with the planet.

[6] Note that the identification of these stars as the largest outliers does not depend on the B07 formulation of gyrochronology. Updating all of the gyro ages to those produced by the (Barnes 2010, hereafter B10) formulation (and adopting the uncertainties from B07, because there is no prescription for calculating uncertainties in B10) yields the same conclusion.

Table 1
Mount Wilson Stars with Suspect Gyrochronology Ages

	HD 45067	HD 89744	HD 107213	HD 187691	HD 212754
$B - V$	0.56	0.54	0.50	0.55	0.52
$P_{\rm rot}$ [day]	8	9	9	10	12
$\log \langle R'_{\rm HK} \rangle$	−5.094	−5.120	−5.103	−5.026	−5.073
$t_{\rm gyro}$ [Gyr]	0.76 ± 0.12	1.11 ± 0.19	1.63 ± 0.33	1.25 ± 0.21	2.30 ± 0.44
$t_{\rm chromo}$ [Gyr]	7.733	8.421	7.966	6.128	7.207
$T_{\rm eff}$ [K]	5973	6149	6249	6059	6210
$\log g$	3.88	3.94	4.13	4.06	3.88
[Fe/H]	−0.19	+0.08	+0.16	+0.04	−0.05
$L/L_\odot$	4.18 ± 0.02	6.38 ± 0.02	5.31 ± 0.02	2.95 ± 0.01	6.72 ± 0.05
MWO $P_{\rm cyc}$ [yr]	Flat	Flat	Long	5.4 (Fair)	Long

References. Barnes (2007); Boeche & Grebel (2016); Gaia Collaboration et al. (2018); Baliunas et al. (1995).

lifetime of a typical F-type star. This argument was used by B07 as justification for giving preference to the gyro ages. However, even if the chromospheric ages are substantially overestimated, the gyro ages are not necessarily correct.

Setting aside questions about the absolute reliability of chromospheric ages, the activity levels certainly suggest that these stars might be significantly evolved (e.g., see Wright 2004). In the bottom half of Table 1, we provide three additional lines of evidence that support this general conclusion. First, we list spectroscopic parameters ($T_{\rm eff}$, $\log g$, [Fe/H]) from Boeche & Grebel (2016). Barnes et al. (2016) argue that gyrochronology has only been calibrated for dwarf stars near solar-metallicity. They classify as subgiants any star with $\log g < 4.2$, and remove from consideration metal-poor stars. By these definitions, all of these Mount Wilson stars would be considered subgiants, and one of them (HD 45067) should be discarded by virtue of its low metallicity. Second, the luminosities shown in Table 1 (Gaia Collaboration et al. 2018) are substantially above the main-sequence luminosity for F-type stars (which is typically less than $2\,L_\odot$). Third, after 25 years of monitoring their chromospheric activity, Baliunas et al. (1995) classified most of these stars as "Flat" (i.e., showing constant activity with fractional variations less than 1.5%) or "Long" (i.e., showing potential variability on a timescale longer than 25 years), suggesting that their global dynamos may have already started to shut down (Metcalfe & van Saders 2017). The one exception is a possible 5.4 yr cycle in HD 187691, which was assigned a false-alarm probability grade of "Fair" by Baliunas et al. (1995). Note that the two solar-type stars near HD 212754 in Figure 1 (HD 178428 and HD 143761) are also classified as "Flat" and "Long." Although there may be substantial problems with chromospheric ages at these low activity levels (e.g., see Mamajek & Hillenbrand 2008), the corroborating evidence in Table 1 of significant evolution suggests that gyro ages may also suffer from systematic errors in this regime.

In the context of our revised picture of magnetic stellar evolution (Section 1), how can we understand this inconsistency between the chromospheric and gyro ages for the Mount Wilson stars in Table 1? As discussed by van Saders et al. (2016), the shutdown of magnetic braking appears to occur at a critical value of the Rossby number ($\mathrm{Ro} \equiv P_{\rm rot}/\tau_c$), the ratio of the rotation period to the convective turnover time. Hotter stars have shallower convection zones with shorter turnover times, so they reach the critical Rossby number at earlier absolute ages while their rotation periods are still relatively short. The result of this transition is a decoupling of rotation and magnetism, with the rotation period remaining almost constant while the chromospheric activity continues to decrease[7] with age (Metcalfe et al. 2016). As suggested by Metcalfe & van Saders (2017), stellar cycles appear to grow longer and decrease their amplitude during this transition before disappearing entirely or becoming undetectable, leading to classifications of "Long" or "Flat" in stellar cycle surveys. With the rotation period essentially fixed, the gyro age is a lower limit that actually reflects the age when the star stopped spinning down in the middle of its main-sequence lifetime.

3. Analogs Observed by *Kepler*

Although asteroseismic observations do not yet exist for the Mount Wilson stars in Table 1 (see Section 4), we can search for analogs of these stars within the sample of *Kepler* asteroseismic targets. There are currently 18 *Kepler* targets with detailed asteroseismic modeling (for precise ages) that also have known rotation periods and measured chromospheric activity (see Metcalfe et al. 2016, their Table 1). Among these stars, only three fall within the same range of rotation periods and $B - V$ colors as the Mount Wilson stars in Table 1. We list the properties of these analogs in the first three columns of Table 2, ordered by activity level.

The chromospheric activity levels for these analogs span the range where the magnetic transition summarized in Section 1 is expected to occur. The critical Rossby number found by van Saders et al. (2016) can also be understood as a critical activity level, because the two properties are strongly correlated (Mamajek & Hillenbrand 2008). The critical activity level is around −4.95 (Brandenburg et al. 2017), so the gap between gyrochronology and other age estimates is expected to grow wider as stars continue to evolve to lower activity levels. We use the $B - V$ color and $P_{\rm rot}$ to calculate gyro ages and uncertainties using the B07 formulation,[8] and we use $\log R'_{\rm HK}$ to calculate chromospheric ages following Donahue (1998). For KIC 9139151, which is just reaching the critical activity level where rotation and magnetism are expected to decouple, the gyro age agrees with the asteroseismic age. For the more

[7] If magnetic energy driven by rotation on large scales is replaced with mechanical energy driven by convection on small scales (Böhm-Vitense 2007), then the change in magnetic morphology that dramatically reduces angular momentum loss need not change the chromospheric activity level abruptly. Recent simulations by Garraffo et al. (2018) support this interpretation.

[8] Ages calculated with the B10 formulation agree with those from B07 within $2\sigma_{\rm gyro}$.

Table 2
Kepler Analogs of the Gyrochronology Outliers

	KIC 9139151	KIC 12009504	KIC 10963065	KIC 10909629
$B - V$	0.520	0.556	0.509	0.540
$P_{\rm rot}$ [day]	10.96 ± 2.22	9.39 ± 0.68	12.58 ± 1.70	12.37 ± 1.22
$\log R'_{\rm HK}$	−4.954	−4.977	−5.054	⋯
$t_{\rm gyro}$ [Gyr]	1.93 ± 0.37	1.06 ± 0.18	2.82 ± 0.57	2.04 ± 0.37
$t_{\rm astero}$ [Gyr]	1.94 ± 0.31	3.44 ± 0.44	4.33 ± 0.30	4.69 ± 0.56
$t_{\rm chromo}$ [Gyr]	4.73	5.15	6.75	⋯
$T_{\rm eff}$ [K]	6302	6179	6140	6265
$\log g$	4.38	4.21	4.29	3.90
[Fe/H]	+0.10	−0.08	−0.19	−0.12
$L/L_\odot$	1.71 ± 0.01	2.71 ± 0.01	1.93 ± 0.01	6.59 ± 0.11

References. García et al. (2014); Metcalfe et al. (2016); Creevey et al. (2017); Serenelli et al. (2017); Buchhave & Latham (2015); *Gaia* Collaboration et al. (2018).

evolved dwarfs KIC 12009504 and KIC 10963065, the gap between the gyro age and the asteroseismic age is significant. The gyro age for these stars appears to indicate the point at which magnetic braking became inefficient and rotation stopped evolving substantially. The available data from *Kepler* suggests that gyrochronology is an unreliable age indicator for hotter stars beyond ∼2–3 Gyr (van Saders et al. 2016).

The chromospheric ages for the analogs appear to be substantially overestimated at these low activity levels, just as with the Mount Wilson stars in Table 1. The other indicators of evolutionary status that are listed in the first three columns of Table 2 generally fall within the range where gyrochronology has been calibrated. The surface gravities are all above the cut ($\log g > 4.2$) suggested by Barnes et al. (2016), only one of the stars (KIC 10963065) is significantly metal-poor, and the *Gaia* luminosities are well below those of the Mount Wilson stars. Most significantly, there is no apparent reason to expect gyrochronology to fail for KIC 12009504, but both the B07 (1.06 Gyr) and B10 (1.10 Gyr) ages are wildly inconsistent with the asteroseismic age (modeling results vary between 3.10 and 4.12 Gyr, Silva Aguirre et al. 2017). If this star is actually too evolved for gyrochronology to be reliable, the rotation period should have *slowed* as it expanded into a subgiant, biasing the gyro age *older* and reducing the inconsistency with asteroseismology.

4. Predictions for *TESS*

The *TESS* mission launched successfully in April 2018, and it is expected to gather short-cadence photometry (2 minute sampling) for all of the Mount Wilson stars listed in Table 1. Detections of solar-like oscillations comparable to what was achieved by *Kepler* are expected in *TESS* targets that are ∼5 mag brighter (Campante et al. 2016). The minimum dwell time on each *TESS* sector is 27 days, comparable to the 30 day time series obtained for *Kepler* targets during the asteroseismic survey that was conducted in the first year (Chaplin et al. 2011b). The amplitude of solar-like oscillations scales with the ratio of luminosity to mass (Houdek et al. 1999), and detections are more likely in magnetically inactive stars (Chaplin et al. 2011a), so the F-type stars in Table 1 should yield asteroseismic data comparable to *Kepler* targets in the magnitude range Kp ∼ 10–11. The 27 day time series should also allow an independent check of the rotation periods determined from the Mount Wilson data.

We searched the García et al. (2014) rotation catalog for the fainter *Kepler* asteroseismic targets that can be considered analogs of the Mount Wilson stars in terms of both stellar properties and the expected data quality from *TESS*. The properties of KIC 10909629, the best *Kepler* analog of HD 212754, are listed in the fourth column of Table 2. KIC 10909629 has a $B - V$ color and rotation period that are both similar to HD 212754, but it is 5.25 mag fainter in the V band. The chromospheric activity level of KIC 10909629 is not known, but the photospheric activity proxy[9] ($S_{\rm ph}$, Mathur et al. 2014) is comparable to that of KIC 10963065, which has $\log R'_{\rm HK} < -5$. The gyro age from B07 (2.04 Gyr) and B10 (2.24 Gyr) are both significantly younger than the asteroseismic age (4.69 Gyr, Serenelli et al. 2017). The spectroscopic parameters and *Gaia* luminosity are similar to those of HD 212754, and support the conclusion that KIC 10909629 is substantially evolved despite its young gyro age. Again, this can be understood if the rotation period of KIC 10909629 stopped evolving after ∼2 Gyr. Based on these results, we predict that asteroseismic ages from *TESS* for the Mount Wilson stars in Table 1 will be significantly older than expected from gyrochronology.

The anticipated quality of the *TESS* observations for the Mount Wilson stars is illustrated in Figure 2. In the top panel, a 27 day segment of the long-cadence *Kepler* observations of KIC 10909629 clearly shows rotational modulation with a period near 12 days and a peak-to-peak amplitude of a few millimagnitudes. In the bottom panel, we show the power spectrum from 390 days of short-cadence data for KIC 10909629 (gray) and for the observations spanning 30 days (blue) that were originally used to detect solar-like oscillations in this star (Chaplin et al. 2011b). In both cases, the signatures of activity, granulation, and shot noise have been modeled and removed using the A2Z pipeline (Mathur et al. 2010). While the longer data set clearly shows the series of evenly spaced frequencies that are characteristic of solar-like oscillations, the shorter time series still reveals a significant power excess ∼900 μHz and a signature of the regular spacing. When combined with spectroscopic parameters, these global properties of the oscillations are sufficient to constrain the stellar age with ∼10%–20% precision (Chaplin et al. 2014; Serenelli et al. 2017).

[9] The photospheric activity proxy can be artificially low for stars when the rotation is viewed nearly pole-on.

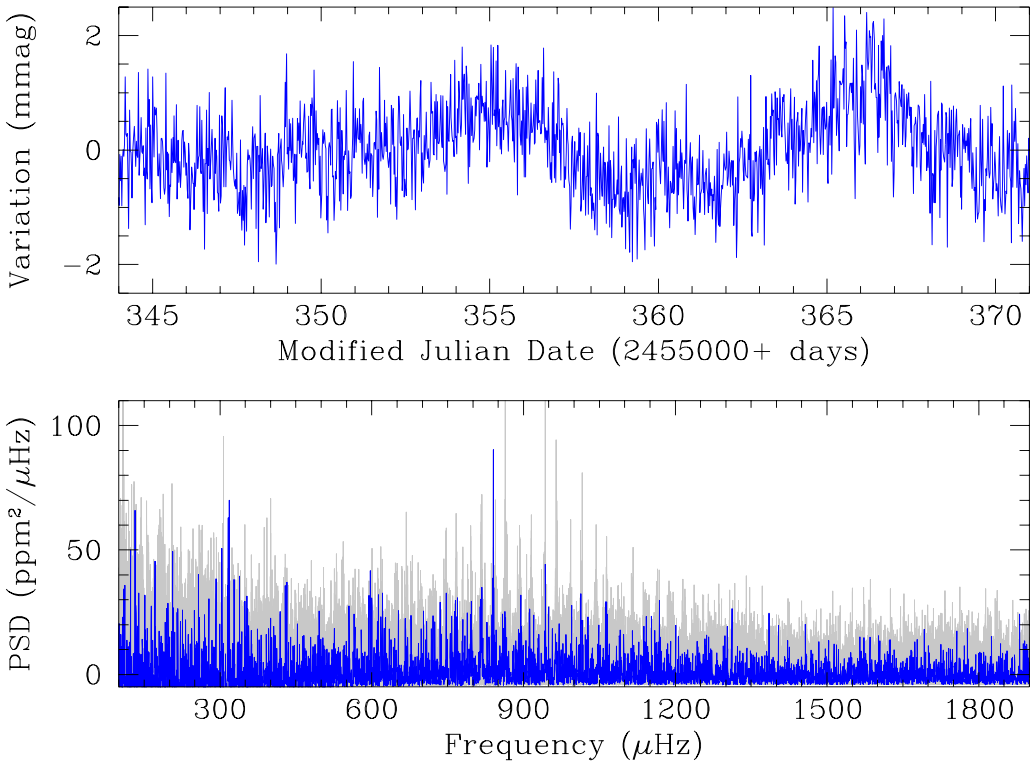

Figure 2. Anticipated quality of *TESS* observations for the Mount Wilson stars listed in Table 1. Top: calibrated 27 day light curve of KIC 10909629, which has a color ($B - V = 0.54$) and rotation period (12.37 days; García et al. 2014) similar to HD 212754. With a *Kepler* magnitude Kp = 10.9, this target yields an S/N comparable to that expected from *TESS* at $V \sim 5.9$. The rotational modulation is apparent, even in this short time series. Bottom: power spectral density from 390 days of short-cadence data for KIC 10909629 (gray) and for the observations spanning 30 days (blue) that were originally used to detect solar-like oscillations (Chaplin et al. 2011b). The signatures of activity, granulation, and shot noise have been removed using the A2Z pipeline (Mathur et al. 2010). The power excess ~900 μHz is significant even in 30 days (Chaplin et al. 2014).

5. Summary and Discussion

After Skumanich (1972) presented observational evidence that stellar rotation rates and magnetic activity levels diminish together over time, the idea of using one or both properties to determine the ages of stars has gradually taken hold. Barnes (2007, 2010) made the idea more quantitative by establishing the mass-dependence and calibrating a gyrochronology relation using young clusters and the Sun. In the absence of additional observations, it was natural to extrapolate these relations to stars beyond the middle of their main-sequence lifetimes. However, over the past few years evidence has emerged that something unexpected occurs in the evolution of stellar rotation and magnetism around middle-age, limiting the utility of gyrochronology relations. When the rotation period of a star becomes comparable to the global convective turnover time, Coriolis forces can no longer sustain the solar-like pattern of differential rotation. The resulting loss of shear disrupts the production of large-scale magnetic field by the global dynamo (Metcalfe et al. 2016). The elimination of large-scale field leads to a dramatic reduction in the efficiency of magnetic braking, so the stellar rotation remains almost constant until the subgiant phase (van Saders et al. 2016, 2018). At the same time the global dynamo gradually shuts down, with the activity cycle period growing longer while the cycle amplitude decreases before disappearing or becoming undetectable (Metcalfe & van Saders 2017).

We have identified the signature of this transition in the observations that were originally used to validate gyrochronology. Using data directly from Barnes (2007, his Table 3), we demonstrate that the most significant differences between chromospheric ages and gyrochronology occur for the most evolved F-type dwarfs (Figure 1). We present several independent lines of evidence to corroborate this interpretation, including surface gravities, Gaia luminosities, and the predominant absence of activity cycles (Table 1). We identify analogs of these F-type stars among the sample of asteroseismic targets observed by *Kepler*, and we show that the asteroseismic ages agree with gyrochronology until a critical activity level ($\log R'_{\rm HK} = -4.95$) beyond which the two estimates diverge (Table 2). Finally, we use observations of a fainter analog from the *Kepler* sample to predict the quality of observations anticipated for these targets from the *TESS* mission, showing that rotation periods and solar-like oscillations should both be detectable (Figure 2). Considering our revised picture of the late stages of magnetic stellar evolution, we predict that these future observations will demonstrate that gyrochronology is unreliable for stars beyond the middle of their main-sequence lifetimes.

There are two key updates to the scenario for magnetic evolution outlined in this paper compared to that proposed by Metcalfe et al. (2016). First, it is now clear that the Rossby number from global convection simulations and that obtained from asteroseismic models that use a mixing-length prescription are not directly comparable (Brun et al. 2017). Based on solar determinations of the Rossby number from both methods, we now believe that the transition near Ro ~ 2 identified by van Saders et al. (2016) corresponds to a change in the

character of differential rotation seen near Ro $\sim$ 1 in convection simulations. In the context of Metcalfe et al. (2016), this implies that stellar evolution across the Vaughan–Preston gap entirely precedes the magnetic transition, which occurs at a substantially lower activity level. Second, there is now observational evidence of possible anti-solar differential rotation in some stars that show higher than expected activity for their rotation rates (Brandenburg & Giampapa 2018). This suggests that when stars reach the critical Rossby number, the differential rotation might flip from solar-like to anti-solar (slow equator, fast poles). Conservation of angular momentum would require the shear to increase, leading to an enhancement of activity in the slowly rotating regime (Karak et al. 2015). Future observations will determine whether this phenomenon represents a temporary phase, or an alternate pathway that coexists with the shutdown of the global dynamo.

While it may be disappointing that rotation is less useful as a diagnostic of age beyond the middle of stellar main-sequence lifetimes, the other Skumanich relation (activity–age) may not be similarly disrupted. Observations of chromospheric activity in a large sample of solar analogs suggest that, unlike rotation, the evolution of activity appears to be continuous across the magnetic transition (Lorenzo-Oliveira et al. 2018). Although the ages adopted for their analysis were derived from isochrones, the *TESS* mission is poised to provide reliable asteroseismic ages for bright stars down to $V \sim 7$ all around the sky. When combined with existing archives of chromospheric activity, it is possible that asteroseismic ages can be used to recalibrate the activity–age relation for older solar-type stars. Given the difficulty of obtaining time series measurements of the diminishing rotational modulation in such stars, and considering that minimal chromospheric variability makes one spectroscopic measurement more likely to be representative of the mean activity level, chromospheric activity might ultimately provide a more reliable age indicator for stars beyond middle-age.

The authors would like to thank Steven Blau, Axel Brandenburg, Hannah Schunker, Andrew Skumanich, David Soderblom, and Jennifer van Saders for helpful exchanges, as well as Rafael García, Savita Mathur, and Warrick Ball for assistance with Figure 2. This research made use of NASA's Astrophysics Data System, as well as the SIMBAD database and the VizieR catalog access tool at CDS in Strasbourg, France. This work benefitted from discussions within the international team "The Solar and Stellar Wind Connection: Heating processes and angular momentum loss" at the International Space Science Institute (ISSI). Support was provided by a Visiting Fellowship at the Max Planck Institute for Solar System Research, and by the Nonprofit Adopt a Star program (adoptastar.org) administered by White Dwarf Research Corporation. R.E. is supported by an NCAR Advanced Study Program Postdoctoral Fellowship. The National Center for Atmospheric Research is sponsored by the U.S. National Science Foundation.

ORCID iDs

Travis S. Metcalfe https://orcid.org/0000-0003-4034-0416
Ricky Egeland https://orcid.org/0000-0002-4996-0753

References

Angus, R., Aigrain, S., Foreman-Mackey, D., & McQuillan, A. 2015, MNRAS, 450, 1787
Baliunas, S., Sokoloff, D., & Soon, W. 1996, ApJL, 457, L99
Baliunas, S. L., Donahue, R. A., Soon, W. H., et al. 1995, ApJ, 438, 269
Barnes, S. A. 2007, ApJ, 669, 1167, [B07]
Barnes, S. A. 2010, ApJ, 722, 222, [B10]
Barnes, S. A., & Kim, Y.-C. 2010, ApJ, 721, 675
Barnes, S. A., Spada, F., & Weingrill, J. 2016, AN, 337, 810
Boeche, C., & Grebel, E. K. 2016, A&A, 587, A2
Böhm-Vitense, E. 2007, ApJ, 657, 486
Brandenburg, A., & Giampapa, M. S. 2018, ApJL, 855, L22
Brandenburg, A., Mathur, S., & Metcalfe, T. S. 2017, ApJ, 845, 79
Brown, B. P., Browning, M. K., Brun, A. S., Miesch, M. S., & Toomre, J. 2010, ApJ, 711, 424
Brun, A. S., Strugarek, A., Varela, J., et al. 2017, ApJ, 836, 192
Buchhave, L. A., & Latham, D. W. 2015, ApJ, 808, 187
Campante, T. L., Schofield, M., Kuszlewicz, J. S., et al. 2016, ApJ, 830, 138
Chaplin, W. J., Basu, S., Huber, D., et al. 2014, ApJS, 210, 1
Chaplin, W. J., Bedding, T. R., Bonanno, A., et al. 2011a, ApJL, 732, L5
Chaplin, W. J., Kjeldsen, H., Christensen-Dalsgaard, J., et al. 2011b, Sci, 332, 213
Creevey, O. L., Metcalfe, T. S., Schultheis, M., et al. 2017, A&A, 601, A67
Donahue, R. A. 1998, in ASP Conf. Ser. 154, The Tenth Cambridge Workshop on Cool Stars, Stellar Systems and the Sun, ed. R. A. Donahue & J. A. Bookbinder (San Francisco, CA: ASP), 1235
Donahue, R. A., Saar, S. H., & Baliunas, S. L. 1996, ApJ, 466, 384
Gaia Collaboration, Brown, A. G. A., Vallenari, A., et al. 2018, A&A, 616, 1
García, R. A., Ceillier, T., Salabert, D., et al. 2014, A&A, 572, A34
Garraffo, C., Drake, J. J., & Cohen, O. 2016, A&A, 595, A110
Garraffo, C., Drake, J. J., Dotter, A., et al. 2018, ApJ, 862, 90
Gastine, T., Yadav, R. K., Morin, J., Reiners, A., & Wicht, J. 2014, MNRAS, 438, L76
Houdek, G., Balmforth, N. J., Christensen-Dalsgaard, J., & Gough, D. O. 1999, A&A, 351, 582
Karak, B. B., Käpylä, P. J., Käpylä, M. J., et al. 2015, A&A, 576, A26
Kuzuhara, M., Tamura, M., Kudo, T., et al. 2013, ApJ, 774, 11
Lorenzo-Oliveira, D., Freitas, F. C., Meléndez, J., et al. 2018, A&A, 619, A73
Mamajek, E. E., & Hillenbrand, L. A. 2008, ApJ, 687, 1264
Mathur, S., García, R. A., Ballot, J., et al. 2014, A&A, 562, A124
Mathur, S., García, R. A., Régulo, C., et al. 2010, A&A, 511, A46
McQuillan, A., Mazeh, T., & Aigrain, S. 2014, ApJS, 211, 24
Meibom, S., Barnes, S. A., Latham, D. W., et al. 2011, ApJL, 733, L9
Meibom, S., Barnes, S. A., Platais, I., et al. 2015, Natur, 517, 589
Metcalfe, T. S., Egeland, R., & van Saders, J. 2016, ApJL, 826, L2
Metcalfe, T. S., & van Saders, J. 2017, SoPh, 292, 126
Miesch, M. S. 2005, LRSP, 2, 1
Noyes, R. W., Hartmann, L. W., Baliunas, S. L., Duncan, D. K., & Vaughan, A. H. 1984, ApJ, 279, 763
Réville, V., Brun, A. S., Matt, S. P., Strugarek, A., & Pinto, R. F. 2015, ApJ, 798, 116
Serenelli, A., Johnson, J., Huber, D., et al. 2017, ApJS, 233, 23
Silva Aguirre, V., Lund, M. N., Antia, H. M., et al. 2017, ApJ, 835, 173
Skumanich, A. 1972, ApJ, 171, 565
Soderblom, D. R., Stauffer, J. R., MacGregor, K. B., & Jones, B. F. 1993, ApJ, 409, 624
van Saders, J. L., Ceillier, T., Metcalfe, T. S., et al. 2016, Natur, 529, 181
van Saders, J. L., Pinsonneault, M. H., & Barbieri, M. 2018, ApJ, submitted (arXiv:1803.04971)
Walker, G. A. H., Croll, B., Matthews, J. M., et al. 2008, A&A, 482, 691
Wilson, O. C. 1968, ApJ, 153, 221
Wright, J. T. 2004, AJ, 128, 1273